2016 23rd International Conference on Telecommunications (ICT)

Robust Low-Complexity Arbitrary User- and Symbol-Level Multi-Cell Precoding with Single-Fed Load-Controlled Parasitic Antenna Arrays

Konstantinos Ntougias, Dimitrios Ntaikos, Constantinos B. Papadias
Athens Information Technology (AIT), 44 Kifissias Avenue, 15125 Maroussi, Greece.
{kontou, dint, cpap}@ait.gr

***Abstract*—In this work, we present a novel technique that enables us to perform robust, low-complexity, arbitrary channel-aware precoding with single-fed load-controlled parasitic antenna arrays. Moreover, we describe the extension of this method to symbol-level and multi-cell precoding scenarios. Finally, we evaluate the sum-rate (SR) throughput performance of multi-cell zero-forcing (ZF) precoding through numerical simulations based on realistic radiation patterns generated by antenna design software as well as on a scattering environment model. Both user-level and symbol-level variants of this precoding method are considered. In addition, a power allocation (PA) scheme which is known for maximizing the SR capacity of coordinated ZF precoding under per base station power constraints is applied in both cases. The simulation results showcase the validity of the proposed approach and illustrate the superiority of symbol-level ZF precoding against its user-level counterpart as well as of the employed PA scheme over the uniform PA method.**

***Index Terms*—Coordinated multiple-input multiple-output (MIMO), parasitic antenna array, inter-cell interference (ICI), multi-cell zero forcing (ZF) precoding, symbol-level precoding.**

I. Introduction

In recent years, multi-user multiple-input multiple-output (MU-MIMO) technology was incorporated in cellular mobile radio communications systems as a means to increase the per-cell spectral efficiency (SE) [1]. MU-MIMO enables the spatial multiplexing (SM) of data streams destined for individual users. The average capacity of the resulting broadcast channel (BC) in the downlink (DL) grows with the number of service antennas, provided that there are at least as many users as transmit antennas [2]. The capacity-achieving transmission strategy is dirty paper coding (DPC), a non-linear multi-user encoding scheme that pre-subtracts the corresponding intra-cell co-channel interference (CCI) prior to transmission [1]. However, its high computational burden makes it impractical. Zero-forcing (ZF) precoding is a popular alternative that offers a good compromise between performance and complexity. This linear precoding scheme employs beamforming (BF) vectors that orthogonalize the users in the spatial domain. Despite its simplicity, ZF becomes optimal as the user population grows at the high signal-to-noise-ratio (SNR) regime [1].

Modern cellular networks adopt universal frequency reuse, in order to enhance the overall SE. Coordinated MIMO has been proposed recently as a means to manage the resulting inter-cell interference (ICI) that limits the system-wide capacity and degrades the cell-edge quality-of-service (QoS). This technology relies on the cooperation between neighboring base stations (BS) to this end. Various cooperation levels with different performance gains and backhaul requirements exist [3].

The aforementioned technologies assume the use of conventional antenna arrays, where active antennas are utilized at the BSs, with each one being fed by a radio frequency (RF) chain. The number of antennas installed at a BS (and, as a consequence, the provided spatial degrees-of-freedom (DoF)) is limited in this case by hardware cost, power consumption, and size constraints [2]. Therefore, there is much interest lately on antenna array paradigms that reduce the required number of RF modules for a target number of DoF and allow the packing of many antennas in a small area, in order to boost the performance of cellular systems.

Load-controlled parasitic antenna arrays (LC-PAA) constitute a representative example [2]. These antenna systems make use of a limited number of active antennas surrounded by a number of passive antennas terminated to tunable loads. They exploit the mutual coupling among the antenna elements caused by the tight inter-element distance to perform adaptive transmit BF by setting the currents on the antennas appropriatelly through the adjustment of the loading values [2]. Single-fed LC-PAAs represent the extreme case where a sole active antenna is utilized. In [4] it is shown that even in this scenario, channel-aware precoding is possible. However, the proposed technique does not support arbitrary precoding, since a stable load combination for the desired precoded signals is not always attainable. [5] proposes a modification of the transmitted signals as a workaround to this problem. Nevertheless, the requirement for computing the appropriate loading values has been proven to be discouraging for the commercial adoption of this antenna technology.

Another interesting remark is that the conventional user-level linear precoding methods aim to reduce or even eliminate CCI. In [6], though, it is demonstrated that at symbol level, CCI may be in some cases constructive, in terms of the received SNR, instead of destructive. Moreover, a symbol-level ZF precoding scheme that predicts the CCI and "zero-forces" only the destructive one, while leaving the constructive inter-

This work has been supported by the EC H2020 Research Project SANSA (grant agreement no: 645047).

978-1-5090-1990-8/16/$31.00 ©2016 IEEE

ference (CI) unaffected, is presented. Numerical simulations show that this method outperforms its user-level counterpart.

In this paper, we describe a technique that enables us to perform robust, low-complexity, arbitrary precoding (both at user- and at symbol-level) with single-fed LC-PAAs. Moreover, we present an extension of this method to multi-cell precoding scenarios. Both ZF and CIZF variants are considered. In addition, we investigate the application of a power allocation (PA) strategy, which is known for maximizing the sum-rate (SR) capacity of multi-cell ZF precoding under per-BS power constraints, to multi-cell CIZF precoding. The simulation is based on realistic beam patterns that have been generated by antenna design software, as well as on a scattering environment model. The numerical simulation results validate the proposed technique and demonstrate the superiority of CIZF precoding against ZF precoding as well as of the considered PA algorithm over uniform PA, in terms of the corresponding SR capacity and achieved SR throughput.

The rest of the paper is organized as follows: Section II introduces the arbitrary channel-aware precoding framework. Section III describes the extension of this technique into multi-cell user-level and symbol-level precoding use cases as well as the employed PA algorithm and the corresponding analytical expressions for SR capacity and throughput. Section IV presents the simulation results. Finally, Section V concludes the paper and presents future research directions.

Notation: a, $\mathbf{a}$, and $\mathbf{A}$ denote a scalar, vector, and matrix. $\mathbb{R}$ and $\mathbb{C}$ denote the set of real and complex numbers. $\mathrm{Re}\,(\cdot)$ denotes the real part of a complex-valued quantity. $|\cdot|$ denotes the magnitude (absolute value) of a complex-valued (real-valued) scalar. a_{ij} represents the element of $\mathbf{A}$ at the ith row and jth column, while a_i denotes the ith entry of $\mathbf{a}$. $(\cdot)^T$, $(\cdot)^\dagger$, $(\cdot)^{-1}$, $(\cdot)^+$, $\mathrm{tr}\,(\cdot)$, and $\mathrm{diag}\,(\cdot)$ denote the transpose, Hermitian transpose, inverse, Moore-Penrose pseudo-inverse, trace, and diagonal of a matrix, respectively, while $\|\cdot\|$ stands for the Euclidean norm of a vector. $\mathbf{I}_n$ and $\mathbf{0}_n$ denote the $n \times n$ identity and zero matrix. $\mathbb{C}^{n\times n}$ represents a $n \times n$ matrix with complex-valued entries. $\mathbb{E}\,(\cdot)$ denotes expectation, $\mathcal{CN}\left(\mu, \sigma^2\right)$ represents a complex-valued random variable (RV) that follows the Gaussian distribution and has mean value μ and variance σ^2, and $\mathcal{CN}\left(\mathbf{M}, \sigma^2\mathbf{I}_n\right)$ represents a complex-valued Gaussian vector whose mean value matrix is $\mathbf{M}$ and its covariance matrix is $\sigma^2\mathbf{I}_n$.

II. Arbitrary Channel-Aware Precoding

In Fig. 1, the equivalent circuit diagram of an M-element single-fed LC-PAA whose parasitic loads have purely imaginary impedance is shown. According to the generalized Ohm's law [4]

$$\mathbf{i} = \left(\mathbf{Z} + \mathbf{Z}_L\right)^{-1}\mathbf{v}, \tag{1}$$

In Eq. (1), $\mathbf{i} \in \mathbb{C}^{M\times 1}$ is the vector of the currents that run on the antenna elements; $\mathbf{Z} \in \mathbb{C}^{M\times M}$ is the mutual coupling matrix whose diagonal entry $Z_{ii} \in \mathbb{C}$ represents the self-impedance of the ith antenna element, while the off-diagonal entry $Z_{ij} \in \mathbb{C}$ denotes the mutual impedance between

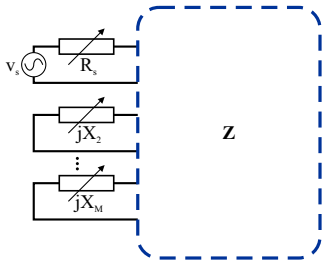

Fig. 1. Equivalent circuit diagram of a single-fed load-controlled parasitic antenna array.

the ith and the jth antenna element $(i, j = 1, 2, \ldots, M)$; $\mathbf{Z}_L \in \mathbb{C}^{M\times M}$ is the diagonal load matrix whose diagonal elements are the source resistance $R_s \in \mathbb{R}$ and the impedances of the parasitic loads $jX_i \in \mathbb{C}$ $(i = 2, 3, \ldots, M)$, where $j = \sqrt{-1}$ is the imaginary unit; and $\mathbf{v} \in \mathbb{C}^{M\times 1}$ is the voltage vector that holds the sole feeding voltage $v_s \in \mathbb{C}$.

Consider a (M, N) MIMO link established between a transmitter and a receiver having M and N antennas, respectively. Regardless of the type of antenna technology used at each end of the link, from an antenna perspective the signal model is given by [4]

$$\mathbf{y} = \mathbf{H}\mathbf{i} + \mathbf{n}, \tag{2}$$

where $\mathbf{y} \in \mathbb{C}^{N\times 1}$ is the vector of the open-circuit voltages at the receive antennas, $\mathbf{i} \in \mathbb{C}^{M\times 1}$ represents the vector of the currents that run on the transmit antennas, $\mathbf{H} \in \mathbb{C}^{M\times M}$ denotes the channel matrix whose entry $h_{nm} \in \mathbb{C}$ relates the mth input current with the nth output open-circuit voltage $(m = 1, 2, \ldots, M;\ n = 1, 2, \ldots, N)$, and $\mathbf{n} \in \mathbb{C}^{N\times 1}$ constitutes a zero-mean circularly symmetric complex Gaussian (ZMCSCG) additive noise vector with covariance matrix $\mathbf{R}_n = \mathbb{E}\left(\mathbf{n}\mathbf{n}^\dagger\right) = \sigma_n^2\mathbf{I}_N$, i.e., $\mathbf{n} \sim \mathcal{CN}\left(\mathbf{0}_N, \sigma_n^2\mathbf{I}_N\right)$. Note that Eq. (2) applies also to the case where the N receive antennas are shared by K users, with each one having a terminal with N_k antennas so that $\sum_{k=1}^{K} N_k = N$.

Eq. (1) implies that in order to perform channel-aware precoding with single-fed LC-PAAs, we have to map the precoded symbols to the antenna currents, that is [7],

$$\mathbf{i} = \mathbf{W}\mathbf{s}, \tag{3}$$

where $\mathbf{W} \in \mathbb{C}^{M\times M}$ is the precoding matrix and $\mathbf{s} \in \mathbb{C}^{M\times 1}$ is the input signal vector. Then, Eq. (2) becomes

$$\mathbf{y} = \mathbf{H}\mathbf{W}\mathbf{s} + \mathbf{n}. \tag{4}$$

In order to apply this channel-aware precoding method in practice, we have to calculate the required currents for the desired precoding scheme and the given input signal according to Eq. (3) and then compute the corresponding loading values according to the generalized Ohm's law in Eq. (1) under the constraint of a positive input resistance in order to avoid circuit instability [8]:

$$\mathrm{Re}\,\{Z_{in}\} > 0. \tag{5}$$

However, the design condition given in Eq. (5) cannot be met for any given input signal constellation or precoding type.

On the other hand, it is well-known that transmit BF with single-fed LC-PAAs does not suffer from this problem, since the desired radiation pattern does not depend on the input signal's format. Based on this remark, we suggest a novel approach for performing *robust, low-complexity, arbitrary channel-aware precoding* with single-fed LC-PAAs. More specifically, we divide the problem to a BF part and a precoding one. That is, we first shape a beam, and then we perform channel-aware precoding over this beam. Thus, we alleviate the complexity associated with the determination of the optimum loading configuration and we overcome the aforementioned challenges regarding circuit stability.

III. Multi-Cell Precoding

In this Section, we present the system setup, the transmission protocol, the system model, the signal models for the considered precoding schemes, the power allocation strategy, and the analytical expressions of SR capacity and throughput.

A. System Setup and Transmission Protocol

We consider the DL transmission in a setup with K cells and one active user per cell. Each BS is equipped with a single-fed LC-PAA with M antenna elements, while the user terminals (UT) have a single antenna. It is assumed that the K BSs can efficiently share channel state information (CSI) and user data over high-speed backhaul / fronthaul links in order to transmit *jointly* using linear precoding to the K UTs[1]. The UTs, on the other hand, operate independently from each other. Each single-fed LC-PAA is able to generate L distinct predetermined beams that correspond to L fixed sets of loading values. Hence, there are L^K possible beam combinations (K-tuples of beams) in total.

At each timeslot, each BS wishes to serve its scheduled user. The K concurrent transmissions take place over the same frequency band. We assume a flat- and block-fading channel model, frequency division duplex (FDD) operation, and unit-variance noise (i.e., $\sigma_n^2 = 1$).

The system operation is divided in three phases:

1) **Learning phase:** For each beam combination, the BSs transmit a pilot signal. Then, the UTs estimate the channel gains related with the cross and direct links and feed them back to their BS.
2) **Beam-selection phase:** Based on the information reported by the UTs, the BSs select jointly the best K-tuple of beams in terms of the achieved SR throughput. (One beam per LC-PAA is selected.)
3) **Transmission phase:** The BSs transmit over the selected beams. CSI feedback allows the application of multi-cell precoding techniques.

The system setup is shown in Fig. 2 for $K = 2$ and $L = 4$.

B. Beam-Selection Criterion

During the learning phase, UT_k estimates the direct channel with BS_k $h_{kk}^{(l)} \in \mathbb{C}$ and the cross channels with the other BSs $h_{km}^{(l)} \in \mathbb{C}$ for each beam combination (l) $\left(k, m = 1, 2, \ldots, K,\ k \neq m,\ l = 1, 2, \ldots, L^K\right)$[2]. The BSs exchange these complex values and compile the composite channel matrix $\mathbf{H}^{(l)} = \left[\begin{array}{cccc} \mathbf{h}_1^{(l)} & \mathbf{h}_2^{(l)} & \cdots & \mathbf{h}_K^{(l)} \end{array}\right]^\dagger \in \mathbb{C}^{K \times K}$ where $\mathbf{h}_k^{(l)} = \left[\begin{array}{cccc} h_{k1}^{(l)} & h_{k2}^{(l)} & \cdots & h_{kK}^{(l)} \end{array}\right]^T \in \mathbb{C}^{K \times 1}$ is the vector of the channel coefficients between UT_k and each BS. Then, the metric $T^{(l)} = \text{tr}\left(\mathbf{H}\mathbf{H}^\dagger\right)^{-1}$ is calculated. After switching through all possible beam combinations, the following beam-selection criterion applies:

CSI-based beam selection criterion: The K-tuple of beams (l) that results in the minimum value of $T^{(l)}$ is selected.

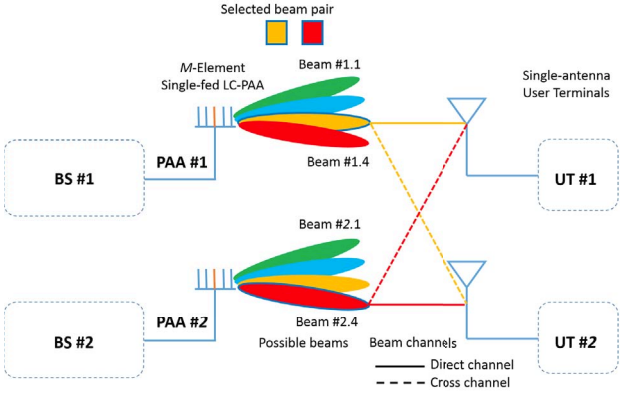

Fig. 2. System model for $K = 2$ and $L = 4$.

C. System Model

The DL transmission over the selected beam combination is described mathematically as[3]

$$\mathbf{y} = \mathbf{H}\mathbf{x} + \mathbf{n}, \tag{6a}$$

$$\begin{bmatrix} y_1 \\ y_2 \\ \vdots \\ y_K \end{bmatrix} = \begin{bmatrix} \mathbf{h_1}^\dagger \mathbf{x} \\ \mathbf{h_2}^\dagger \mathbf{x} \\ \vdots \\ \mathbf{h_K}^\dagger \mathbf{x} \end{bmatrix} + \begin{bmatrix} n_1 \\ n_2 \\ \vdots \\ n_K \end{bmatrix}, \tag{6b}$$

where $\mathbf{y} \in \mathbb{C}^{K \times 1}$ is the vector of the received signals, $y_k \in \mathbb{C}$ is the received signal at UT_k, $\mathbf{n} \in \mathbb{C}^{K \times 1}$ is zero mean circularly symmetric complex Gaussian additive noise vector with covariance matrix $\mathbf{Q}_n = \mathbb{E}\left(\mathbf{n}\mathbf{n}^\dagger\right) = \mathbf{I}_K$, and $n \sim \mathcal{CN}(0, 1)$ is the additive Gaussian noise at UT_k $(k = 1, 2, \ldots, K)$. The transmitted signal vector $\mathbf{x} \in \mathbb{C}^{K \times 1}$ is obtained from the symbol vector $\mathbf{s} = \left[\begin{array}{cccc} s_1 & s_2 & \cdots & s_K \end{array}\right]^T \in \mathbb{C}^{K \times 1}$, where $s_k \in \mathbb{C}$ is the data symbol intended for UT_k, through the following linear transformation:

$$\mathbf{x} = \mathbf{W}\mathbf{P}^{1/2}\mathbf{s}, \tag{7}$$

[1] Perfect CSI is assumed at the BSs.

[2] Note that each BS-UT link is actually a single-input single-output (SISO) channel.

[3] We assume that the effect of path loss and shadowing is captured by the variance of the channel coefficients.

where $\mathbf{W} = \left[\mathbf{w}_1 \;\; \mathbf{w}_2 \;\; \cdots \;\; \mathbf{w}_K \right] \in \mathbb{C}^{K\times K}$ is the precoding matrix, $\mathbf{w}_k \in \mathbb{C}^{K\times 1}$ is the unit-norm BF vector (i.e., $\|\mathbf{w}_k\| = 1$) used to transmit s_k to UT$_k$, and $\mathbf{P} = \text{diag}\left(\sqrt{p_1}, \sqrt{p_2}, \ldots, \sqrt{p_k}\right) \in \mathbb{C}^{K\times K}$ is the power allocation matrix. Hence, Eq. (6a) becomes

$$\mathbf{y} = \mathbf{HWP}^{1/2}\mathbf{s} + \mathbf{n}. \tag{8}$$

The instantaneous signal-to-noise-plus-interference-ratio (SINR) of the kth user is given by

$$\text{SINR}_k = \frac{\left|\mathbf{h}_k^\dagger \mathbf{w}_k\right|^2 p_k}{1 + \sum_{m\neq k}\left|\mathbf{h}_k^\dagger \mathbf{w}_m\right|^2 p_m}, \quad k = 1, 2, \ldots, K. \tag{9}$$

D. Sum-Rate Capacity and Throughput

Assuming Gaussian input, we can express the maximum instantaneous achievable data rate at the kth user as

$$R_k = \log_2\left(1 + \text{SINR}_k\right), \quad k = 1, 2, \ldots, K. \tag{10}$$

Then, the SR capacity is

$$R = \sum_{k=1}^{K} R_k = \sum_{k=1}^{K} \log_2\left(1 + \text{SINR}_k\right). \tag{11}$$

Eq. (11) refers to a hypothetical scenario. In practice, we have finite-alphabet inputs. In this work, we assume for simplicity the use of Binary Phase Shift Keying (BPSK) modulation (i.e., $s_k = \pm 1$, $k = 1, 2, \ldots, K$). In this case,

$$R_k = (1 - \text{BLER})m, \tag{12}$$

where $m = 1$ bit/symbol for BPSK and the block error rate (BLER) is given by $\text{BLER} = 1-(1-P_e)^{N_f}$, with P_e being the symbol / bit error rate (SER / BER) of BPSK and N_f being the frame size. The generalization to higher-order modulation schemes is straightforward.

E. Zero Forcing Precoding

Zero forcing (ZF) precoding nulls the ICI. That is,

$$\left\|\mathbf{h}_k^\dagger \mathbf{w}_m^{(\text{ZF})}\right\|^2 = 0, \quad k, m = 1, 2, \ldots, K, \;\; m \neq k. \tag{13}$$

Hence, the received signal of the kth user can be expressed as

$$y_k = \mathbf{h}_k^\dagger \sqrt{p_k}\mathbf{w}_k^{(\text{ZF})} s_k + n_k, \quad k = 1, 2, \ldots, K. \tag{14}$$

The ZF condition is translated into the use of the Moore-Penrose pseudo-inverse of the composite channel matrix as the precoding matrix:

$$\mathbf{W}^{(\text{ZF})} = \mathbf{H}^{+} = \mathbf{H}^\dagger\left(\mathbf{HH}^\dagger\right)^{-1}. \tag{15}$$

In view of Eq. (13) and since $\sigma_n^2 = 1$, the SINR at the kth user is given by

$$\text{SINR}_k^{(\text{ZF})} = \left\|\mathbf{h}_k^\dagger \mathbf{w}_k^{(\text{ZF})}\right\|^2 p_k, \quad k = 1, 2, \ldots, K. \tag{16}$$

Typically, the precoding matrix is normalized. An often-applied normalization is the following: First, we calculate the matrix $\mathbf{F} = \mathbf{H}^{+}$ and then we divide each column of $\mathbf{F}$ with the norm of this column vector, i.e.,

$$\mathbf{W}^{(\text{ZF})} = \frac{\mathbf{F}(:,k)}{\|\mathbf{F}(:,k)\|}, \quad k = 1, 2, \ldots, K. \tag{17}$$

F. Constructive Interference Zero Forcing Precoding

Let us define the channel cross-correlation matrix $\mathbf{R} \in \mathbb{C}^{K\times K}$ as [6]

$$\mathbf{R} = \mathbf{HH}^\dagger. \tag{18}$$

As described in [6], the symbol-to-symbol ICI from s_k to s_m is expressed as

$$\text{ICI}_{km} = s_k\rho_{km}, \quad k, m = 1, 2, \ldots, K, \;\; m \neq k \tag{19}$$

while the cumulative ICI on s_k from all symbols is given by

$$\text{ICI}_k = \sum_{k=1}^{K} s_k\rho_{km}, \quad m = 1, 2, \ldots, K, \;\; m \neq k \tag{20}$$

where [9]

$$\rho_{km} = \frac{\mathbf{h}_k\mathbf{h}_m^\dagger}{\|\mathbf{h}_k\|\,\|\mathbf{h}_m\|} \tag{21}$$

is the k,m-th element of $\mathbf{R}$ that represents the cross-correlation factor between the kth user's channel and the mth transmitted data stream.

In CIZF, the precoding matrix has the following form [6]:

$$\mathbf{W}^{(\text{CIZF})} = \mathbf{W}^{(\text{ZF})}\mathbf{T} = \mathbf{H}^\dagger\mathbf{R}^{-1}\mathbf{T}. \tag{22}$$

The received signal at the kth user is given by [10]

$$y_k = \tau_{kk}\sqrt{p_k}s_k + \sum_{m\neq k}\text{CI}_{km} + n_k, \quad k, m = 1, 2, \ldots, K \tag{23}$$

where $\text{CI}_{km} = \tau_{km}\sqrt{p_m}s_m$ denotes the constructive ICI from the mth user to the kth user. Then, the kth user's SINR is given by

$$\text{SINR}_k^{(\text{CIZF})} = \sum_{m=1}^{K}\left|\tau_{km}\right|^2 p_m, \quad k = 1, 2, \ldots, K. \tag{24}$$

The matrix $\mathbf{T}$ is calculated on a symbol-by-symbol basis as follows [6]: First, $\mathbf{R}$ is calculated according to Eq. (18) and next, $\mathbf{G} \in \mathbb{C}^{K\times K}$ is computed as

$$\mathbf{G} = \text{diag}(\mathbf{s})\text{Re}(\mathbf{R})\text{diag}(\mathbf{s}). \tag{25}$$

Then, $\tau_{kk} = \rho_{kk}$ and $\tau_{km} = 0$ if $g_{km} < 0$ or $\tau_{km} = \rho_{km}$ otherwise.

G. Sum-Rate Throughput Maximization and Power Allocation

In this work, we make the realistic assumption of per-BS power constraints $p_k \leq P$, where $P \in \mathbb{R}$ is the maximum attainable transmit power (same for all BSs). Moreover, we study not only the scenario of uniform PA but also other PA schemes. More specifically, we apply the water-filling (WF) algorithm described in [11]. Our motivation is that this simple heuristic algorithm is optimum for multi-cell ZF precoding with per-BS power constraints, in terms of the achieved SR throughput, but it can be applied also to other precoding schemes, such as the regularized ZF precoding which introduces a controllable amount of interference.

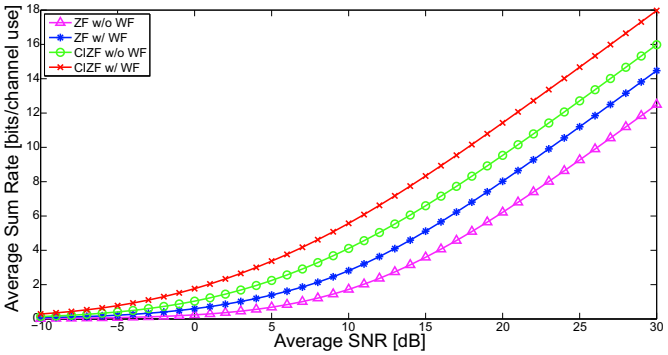

Fig. 3. Numerical simulation results: SR capacity bounds.

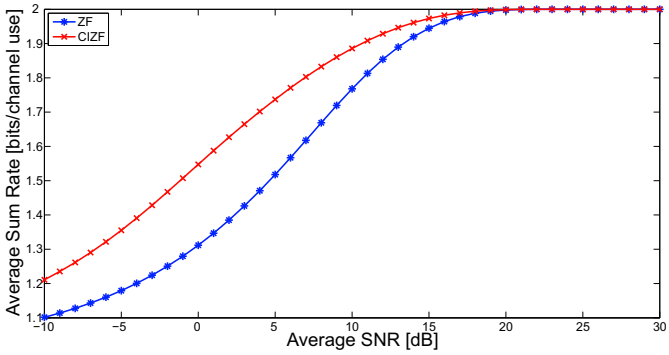

Fig. 4. Numerical simulation results: SR throughput.

IV. Numerical Simulation Results

In this Section, we evaluate the performance of the considered system setup for the use case that is depicted in Fig. 2 through numerical simulations. The performance results represent ergodic SR achieved over target receive SNR values in the range $[-10, 30]$ dB. These results have been obtained after $1,000$ simulation runs by taking the expectation of the corresponding SR equations. A single-bounce scattering model has been incorporated in the simulations to capture the effect of beamforming-based transmission as well as of small-scale and large-scale fading. The beams have a half-power beam width (HPBW) of 30° and correspond to a LC-PAA with $M = 5$ elements. Finally, the channel matrix has been normalized appropriately to facilitate the performance evaluation.

Fig. 3 depicts the SR capacity bounds of the applied precoding techniques. Considering the use case where the PA algorithm described in [11] is employed, we see that CIZF outperforms its user-level counterpart over the entire SNR range of interest, with the difference between the achieved SR growing with SNR at the noise-limited low SNR regime (until $\sim$ 9dB) and then being slowly reduced until it is stabilized in the DoF-limited high SNR regime (from $\sim$15dB and onwards), where ZF is asymptotically optimal. Then, we note that CIZF offers about a 7dB improvement over ZF (while the maximum gain is 9dB). This performance gain is attributed to the fact that CIZF exploits the CI instead of being myopic to the interference type and nulling all kinds of ICI, as ZF does. For comparison purposes, we illustrate also the scenario where no WF is performed, i.e., with a uniform PA strategy. Both precoding schemes perform worse in this case, but the previous arguments still hold.

Finally, Fig. 4 shows the SR throughput performance of these precoding schemes for BPSK input signals and frame size $N_f = 100$. We note that CIZF outperforms ZF precoding. The same performance gain of about 7dB is observed. This gain is reduced with SNR, as in Fig. 3. From 20 dB onwards, these precoding methods perform identical.

Note that for user-level ZF the upper bounds illustrated in Fig. 3 are attainable whereas for CIZF they are just indicative values. In the latter case, the SR thoughput shown in Fig. 4 is the most relevant metric.

V. Conclusion

In this paper, we described a novel approach that enables us to perform low-complexity, arbitrary, robust user- and symbol-level multi-cell precoding with single-fed LC-PAAs. Numerical simulation results based on realistic beam patterns indicated the feasibility of this method as well as the performance gains of symbol-level multi-cell zero-forcing precoding over its user-level counterpart. In the future, we plan to extend this approach to other precoding schemes and to study optimal power allocation strategies.

References

[1] H. Huang *et al.*, Eds., *MIMO Communication for Cellular Networks*. Springer-Verlag New York, 2001.

[2] A. Kalis *et al.*, Eds., *Parasitic Antenna Arrays for Wireless MIMO Systems*. Springer-Verlag New York, 2014.

[3] D. Gesbert *et al.*, "Multi-cell MIMO cooperative networks: A new look at interference," *IEEE Journal on Selected Areas in Communications*, vol. 28, no. 9, pp. 1380–1408, December 2010.

[4] V. Barousis *et al.*, "A new signal model for MIMO communications with compact parasitic arrays," in *IEEE International Symposium on Communications, Control and Signal Processing*, Athens, Greece, May 21-23 2014, pp. 109–113.

[5] L. Zhou *et al.*, "Achieving arbitrary signals transmission using a single radio frequency chain," *IEEE Transactions on Communications*, vol. 63, no. 12, pp. 4865–4878, October 2015.

[6] C. Masouros and E. Alsusa, "Dynamic linear precoding for the exploitation of known interference in MIMO broadcast systems," *IEEE Transactions on Wireless Communications*, vol. 8, no. 3, pp. 1396–1404, March 2009.

[7] G. Alexandropoulos *et al.*, "Precoding for multiuser mimo systems with single-fed parasitic antenna arrays," in *IEEE Global Communications Conference (GLOBECOM)*, Austin, TX, USA, December 8-12 2014, pp. 3897–3902.

[8] V. Barousis and C. B. Papadias, "Arbitrary precoding with single-fed parasitic arrays: Closed-form expressions and design guidelines," *IEEE Wireless Communications Letters*, vol. 3, no. 2, pp. 229–232, February 2014.

[9] M. Alodeh *et al.*, "Constructive multiuser interference in symbol level precoding for the MISO downlink channel," *IEEE Transactions on Signal Processing*, vol. 63, no. 9, pp. 2239–2252, February 2015.

[10] D. Christopoulos *et al.*, "Constructive interference in linear precoding systems: Power allocation and user selection," March 2013, arXiv: 1303.7454.

[11] E. Bjornson and E. Jorswieck, "Optimal resource allocation in coordinated multi-cell systems," *Foundations and Trends in Communications and Information Theory*, vol. 9, no. 2-3, pp. 113–381, January 2013.